High-resolution, hard x-ray photoemission investigation of BaFe$_2$As$_2$: Moderate influence of the surface and evidence for a low degree of Fe $3d$–As $4p$ hybridization of electronic states near the Fermi energy

S. de Jong,[1,*] Y. Huang,[1] R. Huisman,[1] F. Massee,[1] S. Thirupathaiah,[2] M. Gorgoi,[2] F. Schaefers,[2] R. Follath,[2] J. B. Goedkoop,[1] and M. S. Golden[1]

[1]*Van der Waals-Zeeman Institute, University of Amsterdam, NL-1018XE Amsterdam, The Netherlands*
[2]*Helmholz Zentrum Berlin, Albert-Einstein-Strasse 15, 12489 Berlin, Germany*

Photoemission data taken with hard x-ray radiation on cleaved single crystals of the barium parent compound of the MFe$_2$As$_2$ pnictide high-temperature superconductor family are presented. Making use of the increased bulk sensitivity upon hard x-ray excitation, and comparing the results to data taken at conventional vacuum ultraviolet photoemission excitation energies, it is shown that the BaFe$_2$As$_2$ cleavage surface provides an electrostatic environment that is slightly different to the bulk, most likely in the form of a modified Madelung potential. However, as the data argue against a different surface doping level, and the surface-related features in the spectra are by no means as dominating as seen in systems such as YBa$_2$Cu$_3$O$_x$, we can conclude that the itinerant, near-E_F electronic states are almost unaffected by the existence of the cleavage surface. Furthermore, exploiting the strong changes in photoionization cross section between the Fe and As states across the wide photon energy range employed, it is shown that the degree of energetic overlap between the iron $3d$ and arsenic $4p$ valence bands is particularly small at the Fermi level, which can only mean a very low degree of hybridization between the Fe $3d$ and As $4p$ states near and at E_F. Consequently, this means that the itinerancy of the charge carriers in this group of materials involves mainly the Fe $3d$-Fe $3d$ overlap integrals with at best a minor role for the Fe $3d$-As $4p$ hopping parameters and that the states which support superconductivity upon doping are essentially of Fe $3d$ character.

I. INTRODUCTION

The recent discovery of a class of high-T_C superconductors based on (quasi) two-dimensional (2D) FeAs layers, rather than on CuO layers,[1] has caused significant excitement in the field of condensed matter physics. The discovery of a family of superconductors with high transition temperatures, large critical fields, and more isotropic properties than the cuprates also gives a window of opportunity in terms of future applications. Moreover, many hope that these iron pnictides can help us gain more insight into the mechanisms that lead to unconventional superconductivity in general or may even help unravel a now 20-year-old mystery: what makes the high-T_C cuprates superconduct? From the beginning of the cuprate era, surface sensitive probes such as (angle resolved) photoemission spectroscopy [(AR)PES] and scanning tunneling spectroscopy (STS) have played an important role in determining the electronic structure of the high-T_C superconductors.[2,3] Crucial pieces of the high-T_C puzzle have been supplied by these experimental techniques, for instance, insight in the superconducting order parameter and coupling to identifiable bosonic modes.[2] In this light, it will be no surprise that also the iron pnictides are already being studied intensively using the aforementioned techniques.[4–10]

One important point to keep in mind, however, is that the surface electronic structure of a material can differ from the bulk electronic structure, in which case detailed knowledge regarding the origin and nature of these differences is required in order to fully exploit the strong points of techniques such as ARPES and STS to investigate bulk superconductivity.

The pnictides are quasi-two-dimensional materials, such as the cuprates, where one can assign a formal charge to each layer of the crystal structure. As the crystal symmetry at the surface is broken, one can be left with a polar surface and the possibility of having a diverging electrical field at the cleavage plane. To avoid this "polarization catastrophe," the surface of a material can be reconstructed, both structurally and/or electronically. An interesting example of the latter is thought to occur at the interface of perovskite heterostructures, such as LaAlO$_3$/SrTiO$_3$. Such heterointerfaces are conducting,[11] although both oxides have a band gap of several electron volts. The diverging electrical field is quenched here by means of a partial charge transfer, giving the interface layer half the charge and opposite sign with respect to the charge of the layer below.

In order to compare the surface and bulk properties of a material one would want to be able to tune the probing depth of the experiment. In a photoemission experiment the escape depth of the photoelectrons is sensitive to their kinetic energy, i.e., the excitation energy of the photons. Conventional (AR)PES experiments are performed with photon energies typically between 20 and 100 eV [in the (vacuum) ultraviolet (VUV) range], coinciding with a minimum in the electron escape depth and thus probing only the first few angstroms below the surface. By choosing higher excitation energies in the hard x-ray regime ($h\nu$'s of several keV), the probing depth is increased to nanometers or even tens of nanometers.

In this paper, we present results from a photoemission study of the undoped parent compound of one of the main pnictide high-T_C superconductor families, BaFe$_2$As$_2$ (abbreviated forthwith as Ba122), presenting core-level and
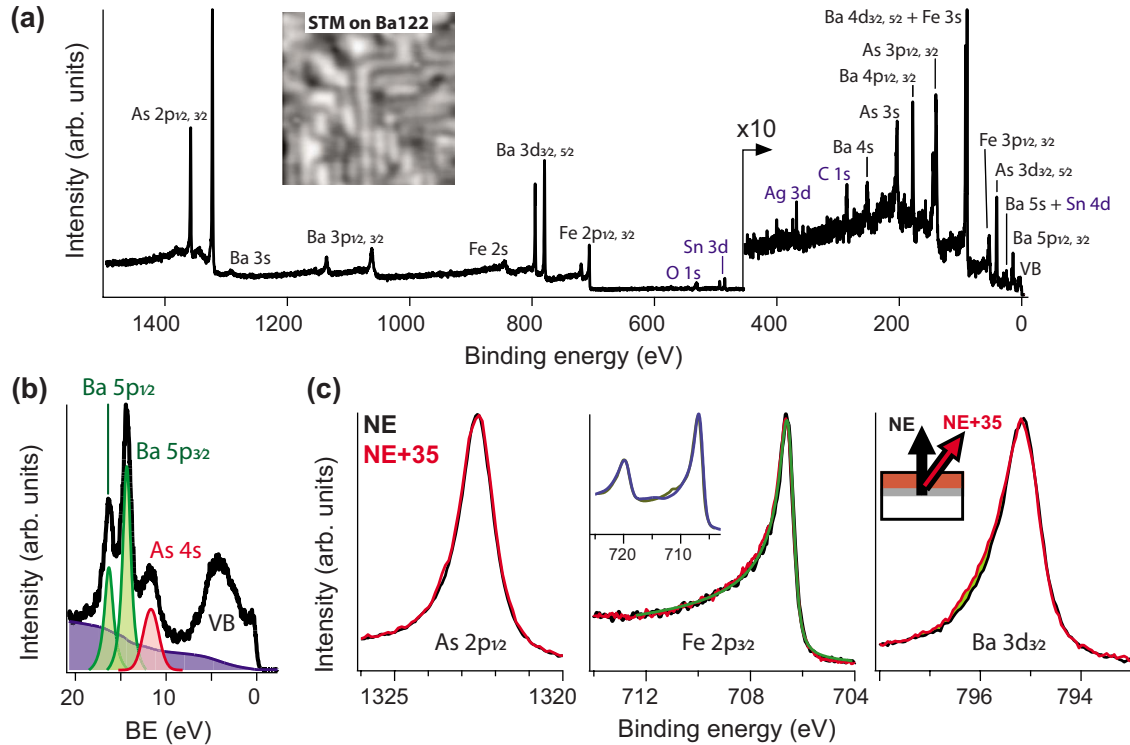
FIG. 1. (Color online) Hard x-ray photoemission data from Ba122. All data taken at room temperature. (a) Overview spectrum taken with $h\nu=3000$ eV. The inset shows a scanning tunneling microscopy topograph (150×150 Å^2) from room-temperature cleaved Ba122, displaying a clear surface reconstruction that lacks long-range order [taken from Ref. 14]. (b) Zoom of the near valence-band region displaying the Ba 5p (green shaded) and As 4s core levels (red shaded) and an approximate inelastic background in blue. Representative core-level spectra ($h\nu=2010$ eV) for all three elements are shown in (c). Displayed are spectra taken in a normal emission geometry (black) and 35° off normal (red), the latter decreasing the bulk sensitivity, as the mean-free path length of the electron is determined by the photon energy and the escape depth thus by the emission angle (illustrated schematically in the inset of the rightmost panel). The Fe $2p_{3/2}$ peak is fitted with a single Doniac-Sunjic line shape, displayed in green. Note that the normal and off normal recorded spectra for As $2p$ and Fe $2p$ fall exactly on top of each other, but that the off normal recorded spectrum for Ba $3d$ has additional spectral weight on the high binding energy side. The inset to the Fe $2p_{3/2}$ core-level spectrum shows a broadened and background corrected version of this spectrum including the Fe $2p_{1/2}$ line (blue) together with Fe $2p$ core lines from metallic Fe(111) taken from Ref. 15 in green. Note the excellent resemblance. For the Ba $3d_{3/2}$ line shown in the rightmost panel of (c), the difference between normal and off-normal emissions is highlighted in green. Note that the normal and off normal recorded spectra for As $2p$ and Fe $2p$ fall exactly on top of each other, but that the off normal recorded spectrum for Ba $3d$ has additional spectral weight on the high binding energy side.

k-integrated valence-band (VB) spectra for this composition. Ba122 has been reported to become superconducting by both hole doping (substituting K for Ba) and electron doping (substituting Co for Fe), with a maximum T_C of 40 and 22 K, respectively.[12,13]

Reports in the literature have pointed out that the cleavage plane of single crystalline Ba122 is most likely to be the Ba block layer.[8,14] As this compound consists of FeAs layers separated by a *single* Ba layer, this means that (in order to obtain a symmetric cleave and maintain charge neutrality) the top barium layer on the surface termination after the cleave should contain half the number of atoms compared to the bulk Ba layers. The surface of Ba122 is thus expected to differ from the bulk, structurally. This has been shown to be the case by several groups doing scanning tunneling microscopy, where a clear reconstruction of the tetragonal unit cell is visible.[8,10,14] The nature of the reconstruction has been reported to be 2×1,[10] or with larger period,[14] but upon cleavage at room temperatures it lacks sufficient long-range

order to be observed using low energy electron diffraction.[14] An example of such a disordered, reconstructed Ba122 surface is shown in the inset of Fig. 1(a). The question is, of course: what will be the effect of these specifically surface-related phenomena on the electronic structure of the surface and near surface region?

By comparing photoemission measurements carried out using hard x-ray radiation and data taken at conventional excitation energies, we find that the former give information mainly about the bulk electronic structure of Ba122, while the latter data show signs of an additional surface electronic structure component, representing a minor alteration of the electronic environment at the termination surface compared to the bulk. We can therefore conclude that the surface of this parent compound of the pnictide 122 high-T_C superconductors is electronically reconstructed with respect to the bulk electronic structure but that the deviation from the bulk situation is modest. The implications of this altered surface

structure are expected to be small for the near-E_F electronic states.

Having clarified this point, we are able to use data recorded with widely differing photon energies to show that the majority of the As $4p$ and Fe $3d$ states that make up the VB of Ba122 possesses relatively little overlap in energy. This means that the degree of hybridization between iron $3d$ and arsenic $4p$ orbitals is quite small for this compound compared to the Cu-O hybridization in the high-T_C cuprates. Importantly, the near-E_F states are almost exclusively Fe $3d$; thus, the hopping of the itinerant charge carriers in this parent compound of the pnictide high-temperature superconductors involves mainly the Fe $3d$-Fe $3d$ overlap integrals.

II. EXPERIMENT

Experiments with photon energies $h\nu$=2010 and 3000 eV were performed at the KMC-1 beamline at the Helmholtz-Zentrum Berlin, coupled to the *Scienta* R4000 analyzer of the HiKE end station.[16] Experiments were carried out at room temperature in a grazing incidence geometry with a total energy resolution of 300 and 450 meV for $h\nu$=2010 and 3000 eV, respectively, as determined from the width of the Fermi edge of a piece of gold foil. Single crystals of Ba122 larger than 1×1 mm^2 were grown from Sn flux and cleaved in a vacuum better than 1×10^{-9} mbar, resulting in shiny, flat cleavage surfaces. The level of tin impurities in the crystals was estimated from core-level intensities to be on the order of 7 at. %, and these single crystals show a magnetic and structural transition at a reduced temperature of 60 K, instead of the familiarly observed 140 K for Sn impurity-free samples.[13]

Experiments with $h\nu$=125 and 140 eV were carried out at the UE112–PGMa beamline at the Helmholtz-Zentrum Berlin using an SES100 electron analyzer and were performed both at room temperature and at low temperature (25 K), with an experimental energy resolution of 30 meV. These experiments were performed on the same batch of single crystals as the HiKE experiments and on the sample surfaces cleaved both at room and at low temperatures in a vacuum better than 2×10^{-10} mbar. The results obtained did not depend on the temperature at which the crystal was cleaved. Spectra were taken in transmission (k integrating) mode of the electron energy analyzers.

III. HARD X-RAY DATA

In Fig. 1(a) an overview spectrum of Ba122 taken with $h\nu$=3 keV is shown, displaying many core-level lines. The small O $1s$, C $1s$, and Ag $3d$ signals come from surface contamination of the sample holder and the silver loaded epoxy that was used to attach the Ba122 crystal to the sample holder.[17] The binding energies of identifiable core levels are listed in Table I. Figure 1(b) shows a zoom of the near-E_F region with clearly distinguishable, spin-orbit split Ba $5p$ lines at a binding energy (BE) of 15 eV, the As $4s$ line at 12 eV and the VB between BE$\approx$8 eV and E_F. We note that the As $4s$ line at 12 eV has been confused in the literature with a charge transfer satellite coming from the Fe $3d$ states of the

TABLE I. Binding energies (BE) in eV of the measured core levels of Ba122, $h\nu$=3000 eV, T=room temperature. The Fermi level was determined from the Fermi cutoff of piece of gold foil. The accuracy of the binding energy determination is ±100 meV. The Fe $3s$ line coincides with the Ba $4d$ lines and could thus not be resolved. The Fe $3p$ spin-orbit splitting could also not be resolved.

Core level	BE (eV)	Core level	BE (eV)
As $2p_{1/2}$	1358.1	Ba $4p_{3/2}$	178.1
As $2p_{3/2}$	1322.4	As $3p_{1/2}$	145.0
Ba $3s$	1292.8	As $3p_{3/2}$	140.1
Ba $3p_{1/2}$	1136.0	Fe $3s$	
Ba $3p_{3/2}$	1062.1	Ba $4d_{3/2}$	92.0
Fe $2s$	844.9	Ba $4d_{5/2}$	89.5
Ba $3d_{3/2}$	795.1	Fe $3p_{1/2,3/2}$	52.7
Ba $3d_{5/2}$	779.7	As $3d_{3/2}$	41.4
Fe $2p_{1/2}$	719.6	As $3d_{5/2}$	40.7
Fe $2p_{3/2}$	706.5	Ba $5s$	29.6
Ba $4s$	252.9	Ba $5p_{1/2}$	16.3
As $3s$	204.2	Ba $5p_{3/2}$	14.4
Ba $4p_{1/2}$	192.2	As $4s$	11.6

valence band.[18] This spectral feature however is unlikely to originate from a satellite as its spectral weight at $h\nu$ =3 keV is comparable to the entire valence band. At lower excitation energies its relative weight becomes significantly smaller; see for instance the inset of Fig. 2(b) taken with $h\nu$=125 eV. The spectral weight of the 12 eV feature traces the tabulated photoionization As $4s$ cross-section values[20] for these two photon energies, thus supporting an assignment to the As $4s$ shallow core level.

Figure 1(c) shows spectra of representative core levels from the three elements in Ba122: As $2p$, Fe $2p$, and Ba $3d$, taken with a photon energy of 2010 eV. Comparing the line shapes of the three core levels, it is immediately clear that while the As $2p$ and Ba $3d$ peaks are quite symmetric, the Fe $2p$ line is not. The Fe $2p$ peak can be fitted with a single Gaussian-broadened Doniac-Sunjic line shape with asymmetry parameter α=0.44, a value that is identical to reported values for elemental Fe.[15] If the asymmetry in the Ba122 Fe core lines was caused by the presence of high BE charge transfer satellites, one could expect the signature of a shoulder in the spectrum, but instead the high BE side of the core line is completely smooth. The inset in Fig. 1(c) shows the measured Fe $2p$ spectrum together with a Fe(111)$2p$ line from the literature.[15] The measured spectrum has been broadened with a Gaussian with full width of half maximum (FWHM=700 meV to compensate for the higher resolution of our experiment, and additionally a smooth Shirley-type background has been subtracted from the hard x-ray excited data presented here so as to enable a reasonable comparison of the two spectra. One can see that the two spectra coincide perfectly.[21] The fact that the Ba122 Fe core-level lines are so identical to those of elementary Fe means that the asymmetry of the core lines is best though of as caused by the significant partial density of states (pDOS) of Fe at the Fermi level. This

(a)

(b)
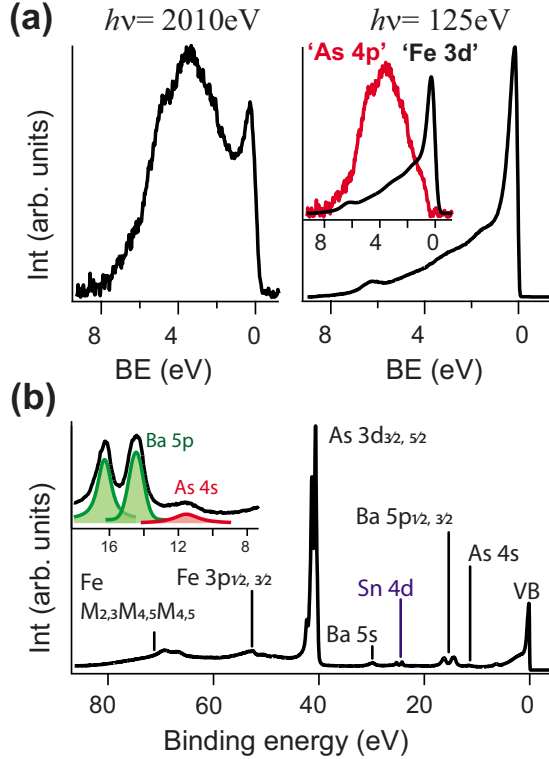
FIG. 2. (Color online) Comparison of x-ray and VUV photo-emission valence-band data (a) Valence-band spectra taken with $h\nu=2010$ eV, $T=$room temperature and $h\nu=125$ eV, $T=20$ K (Ref. [19]). The inset shows a broadened version of the $h\nu=125$ eV spectrum, representing the Fe $3d$ pDOS of the valence band. This curve has been subtracted from the one in the left panel to obtain the As $4p$ pDOS (shown as the red curve in the inset). (b) Shallow core levels of Ba122 recorded with $h\nu=125$ eV, $T=20$ K. The inset shows a zoom of the Ba $5p$ and As core levels, with their Lorentzian peak fits (green shaded and red shaded areas, respectively).

enables a continuum of possible excitations during the creation of the core hole, leading to a smooth "loss tail" at the high BE side of the core-level line. In turn, the fact that the As $2p$ core line in Fig. 1(c) is so symmetric (a fit with a Doniac-Sunjic line form yields an α of only 0.06) means that the As pDOS at the Fermi level is almost negligible in comparison with the Fe $3d$ contribution. The core-level lines were recorded both in normal emission geometry, as well as with an emission angle of 35° off normal. The latter geometry increases the surface sensitivity of the experiment [see the inset in Fig. 1(c)] but yields almost identical results as normal emission for the Fe $2p$ and As $2p$ core lines. The Ba $3d$ line, however, is broader when recorded in off-normal emission, as can be seen in the rightmost panel of Fig. 1(c). Although the difference is quite small, it is evident that there is a small surface contribution for the Ba core lines, causing a (modest) asymmetry in the Ba $3d$ line shape.

IV. VALENCE-BAND DATA

Now focusing on the near E_F electronic states, a zoom of the valence-band region taken with $h\nu=2010$ eV is depicted

in Fig. 2(a). One can see that the total bandwidth of the valence band is about 6–8 eV, displaying a sharp peak close to E_F (the maximum being centered at about 350 meV BE) and a broad hump between 3 to 7 eV. From our core-level data it is already evident that the DOS closest to E_F consists primarily of Fe $3d$ states, but at this particular photon energy ($h\nu=2010$ eV), the photoionization cross sections (PIXs) (Ref. [20]) for Fe $3d$ and As $4p$ are roughly equal, meaning that we cannot *a priori* distinguish between Fe and As pDOSs. At photon energies around 100 eV however, the PIXs favor Fe $3d$ with respect to the As $4p$ states by a factor 70, making spectra measured with these photon energies representative for the Fe $3d$ pDOS. In Fig. 2(a) one can also see a valence-band spectrum recorded with $h\nu=125$ eV,[22] with a large peak at E_F and hardly any sign of a hump at higher binding energies, showing that the Fe $3d$ states are indeed located close to or at E_F and that the As $4p$ states are mainly responsible for the spectral weight between 3 and 7 eV. The inset in Fig. 2(a) shows the difference between the measured spectra in panel (a) whereby the $h\nu=125$ eV spectrum has been broadened with a Gaussian of 350 meV to account for the difference in resolution and temperature between the two measurements. This subtraction spectrum gives an estimate for the As $4p$ density of states. One minor remark is that the relative spectral weight of the As $4p$ to the Fe $3d$ states would then be roughly 2:1 for the hard x-ray data, judging from the area under the curves in the inset of Fig. 2, which is a factor of 2 too high if compared to tabulated photoionization cross sections. These cross sections however are listed for atomic values, and it is not certain that they are strictly applicable to the valence band of a material such as Ba122. The important, qualitatively robust point we make here is that there is little overlap in energy between the main maxima of the Fe $3d$ (350 meV) and the As $4p$ states (4 eV). In the literature, several studies, both theoretical[23] and experimental,[24] have suggested that the Fe $3d$ and As $4p$ states are strongly hybridized, thereby trying to rationalize the small measured Fe magnetic moment compared to predictions from local-density approximation (LDA) calculations. Others, however, have argued that the Fe-As overlap is small.[25] Although from our data it is hard to make a quantitative statement about the hybridization between Fe and As, it is clear that electronic states between E_F and the first 1.5 eV, which determine the physical properties such as magnetism and superconductivity, are (almost) exclusively of Fe $3d$ character. This would not mean the As $4p$ states are of no importance: our data would not exclude an important role for the As atoms as a source of screening of the iron on-site Coulomb repulsion.[25] We stress here that our use of the Ba122 compound enables us to draw these conclusions regarding the Fe-As covalence in a reliable manner. Many photoemission studies in the literature have been carried out on the structurally related 1111-pnictides[24,26,27] that, besides arsenic, also contain oxygen. The O $2p$ states of these compounds overlap in energy with the As $4p$ states[25,28] and give a strong contribution to the valence-band spectral weight, both at low as well as at high photon energies, thus making a trustworthy disentanglement of the As and Fe partial density of states practically impossible.
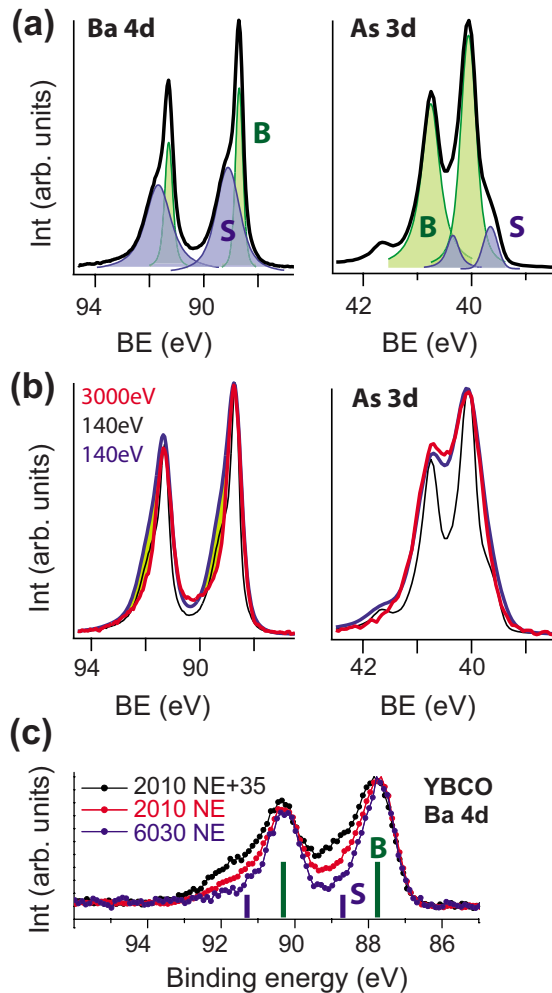
FIG. 3. (Color online) Surface versus bulk electronic states of Ba122 from comparison of x-ray and VUV photoemission data; (a) Ba $4d$ (left) and As $3d$ (right) core levels recorded with $h\nu=140$ eV (black). The surface (S), and bulk (B), contributions have been determined by a fit with four Gaussian-broadened Lorentzians and are shown with blue and green shaded areas, respectively. (b) For comparison, the same core levels recorded with $h\nu=3000$ eV (red) are shown together with the data from panel (a) (thin black) and Gaussian-broadened versions of the latter (blue) to compensate for the difference in experimental resolution. (c) Ba $4d$ core levels of cleaved YBa$_2$Cu$_3$O$_x$ ($x=6.75$) taken with different experimental geometries and photon energies in the hard x-ray regime. Data shown courtesy of Maiti and co-workers. Note the large spectral weight of the surface contribution here and the large energy difference between bulk (b) and surface (s) states, indicated in the figure with green and blue vertical lines, respectively.

V. SHALLOW CORE-LEVEL DATA

Now zooming in on the form of the As $3d$ and Ba $4d$ levels, it is evident that for both core levels the main lines have shoulders [see panel (a) of Fig. 3], taken with $h\nu=140$ eV. The weight of these features varies slightly from cleavage surface to cleavage surface. Note that whereas the shoulder of the As $3d$ line is always located at the low binding energy side of the main line, the Ba $4d$ shoulders are

reproducibly situated at the high binding energy side of the main line. The size of the binding energy shift for both elements is similar: $+(-)400$ meV for Ba (As). The appearance of these extra core-level features is most naturally explained in terms of the existence of surface and bulk contributions. The relative weight of these contributions has been determined by fitting the spin-orbit split doublets with, in total, four Gaussian-broadened Lorentzians, for both the As $3d$ and the Ba $4d$ core levels. We mention in passing that the spin-orbit splitting of the As $3d$ core level is 670 meV, which is very close to the value found for metallic arsenic,[29] and thus we are of the opinion that this value itself cannot be taken as a signal of strong Fe-As hybridization, as was done recently in a photoemission study of a member of the 1111-pnictide family.[24]

From Fig. 3(a) one can see that with respect to that of As, the surface contribution for Ba is very large and significantly broadened when compared to the bulk states, which would support a picture in which the Ba atoms indeed make up the termination surface after UHV cleavage of Ba122 single crystals. The broad energy distribution of the Ba surface states might partly be due to adsorption of residual gas from the vacuum onto the surface, or, more significantly, to the absence of long-range structural order in the topmost Ba layer [as shown in the inset in Fig. 1(a)].[10,14] The fact that the surface contribution for arsenic is much more narrow than for Ba can also be rationalized within the same picture as the "subsurface" As layer is far less perturbed by the cleavage and possesses a markedly reduced variation in electronic environments compared to the topmost Ba layer. Furthermore, the small spectral weight of the surface features in the As spectra compared to the Ba case can be taken as evidence that the effect of the presence of the surface is rapidly screened away for the atomic layers further below the Ba termination layer.

In Fig. 3(b) the same core-level spectra as in panel (a) are plotted, overlain with the same core levels measured with $h\nu=3$ keV. It is evident that the (much more surface sensitive) $h\nu=140$ eV data for Ba $4d$ (left panel) are much broader at the base, although they were recorded with much higher resolution than the hard x-ray data. Broadening of the VUV-excited Ba $4d$ data, to correct for the difference in experimental resolution, gives an asymmetric line shape with much more spectral weight at the high binding energy side than the $h\nu=3$ keV data, emphasizing the fact that the hard x-ray data is indeed probing the electronic structure representative for the bulk of Ba122. The As $3d$ peaks, as measured with $h\nu=140$ eV, are significantly narrower compared to the x-ray data, and broadening yields a spectrum that is, despite the non-negligible surface component, almost identical to the 3 keV data. This also explains why the surface contribution for As could not be resolved from comparison between the 3 keV and 2010 eV x-ray data, while it was evident for the Ba core levels. Also the Fe $3p$ core level (not shown) shows an altered peak form when measured with $h\nu=140$ eV compared to the hard x-ray data, although the VUV-excited signal is very weak and thus not amenable to further analysis. In addition, the small spin-orbit splitting and the Doniac-Sunjic peak form for this line disqualify a disentanglement of the surface and bulk contributions for the Fe $3p$ signal.

An important point to unravel is, of course, the exact origin of the difference between the surface and the bulk electronic environments of Ba122. In general, the shift of a core level ΔE can be explained by a number of terms given by the following formula:

$$\Delta E = \Delta \mu + K \Delta Q + \Delta V_M - \Delta E_R,$$

where $\Delta \mu$ is the change in the chemical potential, ΔQ is the change in the number of valence electrons of the atom under consideration, ΔV_M is the change in the Madelung potential, and ΔE_R is the change in the extra-atomic relaxation energy due to polarizability of the atoms and the conduction electrons surrounding the created core hole.[30] In the case of Ba122 it is a nontrivial exercise to determine exactly the role played by each of these terms at the surface. One may expect, at least, that the polarization and the Madelung potential are different at the surface, although it is difficult to disentangle these two contributions. A good starting point would therefore be to compare the measured data for Ba122 to a known case from the literature in which (electronic) surface renormalization is known to play an important role.

Let us first consider the possibility of a (grossly) different charge carrier concentration at the surface, i.e., an altered surface doping level. From photoemission investigations it is known that certain cuprates which lack a natural cleavage plane, such as $YBa_2Cu_3O_x$ ($x \approx 7.0$)—YBCO for short—show such a surface doping effect.[31] For YBCO this is caused by the fact that the CuO chains are ruptured upon cleavage, remaining behind—in the form of debris—on the termination surface. These chain fragments donate extra holes to the underlying copper-oxygen plane bilayer. The analogy with Ba122, where also only half of a bulk crystal layer remains on the surface after cleavage, is obvious. This type of electronic surface reconstruction for YBCO, however, has a drastic effect on the measured core-level spectra, as can be seen in Fig. 3(c). Depicted are Ba 4*d* core levels taken, in order of decreasing bulk sensitivity, with $h\nu \approx 6$ keV and $h\nu \approx 2$ keV in normal emission geometry and $h\nu \approx 2$ keV with 35° off-normal emission. The difference between spectra recorded with the latter two sets of experimental conditions is still very significant, showing that one has a sizable surface contribution even with an excitation energy of 2 keV. This is not the case for Ba122 [Fig. 1(c)], where the difference between normal and off-normal emissions is nigh indistinguishable. Also, the shift of the surface states of YBCO is quite large: about 1 eV with respect to the bulk states, more than twice that seen in Ba122. Moreover, the increased surface doping of YBCO leads to a shift of surface states toward higher binding energy both for the cations and anions (O^{2-}), so this mechanism can most likely be disqualified as the cause of the electronic surface reconstruction of Ba122.

The picture for Ba122 shown in Fig. 3(a) is, in fact, very reminiscent of the situation seen in x-ray photoemission from the GaAs (110) surface, where the core levels are known to contain a surface contribution.[32] This surface component has a shift in binding energy (with respect to the main line) that is opposite for the negatively and positively charged As and Ga ions: toward lower and higher binding energies, respectively. This shift has been explained by a change in the Madelung potential at the surface[33] with a core-level shift that happens to be close to what we find here for Ba122. Therefore, it is quite credible that the altered surface electronic structure of Ba122 is caused by a change in the Madelung potential, with the surface doping level itself being very close or equal to the bulk value for the Ba122 material. The question then arises as to what effect this has on the valence-band states and, in particular those close to E_F, which are intimately involved in the superconductivity in the doped Ba122 and related materials.

First, while one may expect the altered surface Madelung potential to have some effect, one should bear in mind that the near-E_F states in these systems are bandlike and itinerant in nature, whereas the concept of a Madelung energy is more generally applicable to localized, ionic electronic levels. Second, in the case of GaAs (which possesses a band gap on the order of 1 eV), calculations have indicated that the presence of occupied surface electronic states are attributable to the altered Madelung potential in that system, lying at about 500 meV below the valence-band edge. Yet, no sizable, structured contribution from these states has been identified in photoemission experiments.[34] Taking all these considerations together, we conclude that the near-E_F electronic structure at the surface of Ba122 is very close to that of the bulk. Furthermore, the fact that the surface doping level of Ba122 looks to be the same as the bulk (despite the presence of a reconstructed and potentially polar Ba termination layer) provides confidence that STM and ARPES should be representative probes to investigate the bulk properties of Ba122, such as spin ordering transition temperatures and superconductivity, both in terms of critical temperature and superconducting gap sizes as a function of temperature and doping.

VI. CONCLUSIONS

We have presented high-resolution photoemission data taken with hard x-ray and VUV photon beams on single crystals of the undoped parent compound of the electron- and hole-doped pnictide high-temperature superconductor, $BaFe_2As_2$. From the line shape of the core levels it could be deduced that the near-E_F electronic states are primarily of itinerant Fe 3*d* character. By comparing the hard x-ray excited data with results obtained using conventional VUV excitation energies, we were able to disentangle the approximate Fe and As partial densities of states in the valence band and show that the contribution of the As 4*p* states near the Fermi level is very small indeed. Seeing as this energy region is where the Fe 3*d* partial density of states is maximal, this strongly suggests that the degree of hybridization between the Fe 3*d* and As 4*p* states is minimal at and near E_F for these states, a fact that could be of considerable significance in relation to the issue of the small magnetic moment found at the Fe sites in these compounds.

The exploitation of two widely differing regimes of photoelectron kinetic energies has also enabled us to examine whether the electronic structure of the cleaved Ba122 surface is the same as or close to that of the bulk. By comparison with the well-studied case of GaAs, we find that the termi-

nation surface—which comprises the Ba layer of the quasi-2D crystal structure—is likely to possess a modified Madelung potential, compared to the bulk. However, the core-level data do provide evidence against the existence of a surface region with differing doping level. The departure of the surface contribution to the electronic structure in Ba122 from the bulk situation is very modest in the iron pnictide. Therefore, the distorting effects of the real cleavage surface on the investigation of bulk representative near-E_F electronic properties of Ba122 and related compounds with surface sensitive probes such as angle resolved photoemission and scanning tunneling spectroscopy are found to be minor in nature.

*sdejong@science.uva.nl

[1] Y. Kamihara, T. Watanabe, M. Hirano, and H. Hosono, J. Am. Chem. Soc. **130**, 3296 (2008); Ren Zhi-An, Lu Wei, Yang Jie, Yi Wei, Shen Xiao-Li, Zheng-Cai, Che Guang-Can, Dong Xiao-Li, Sun Li-Ling, Zhou Fang, and Zhao Zhong-Xian, Chinese Phys. Lett. **25**, 2215 (2008).

[2] A. Damascelli, Z. Hussain, and Z.-X. Shen, Rev. Mod. Phys. **75**, 473 (2003).

[3] Ø. Fischer, M. Kugler, I. Maggio-Aprile, C. Berthod, and C. Renner, Rev. Mod. Phys. **79**, 353 (2007).

[4] D. H. Lu, M. Yi, S.-K. Mo, A. S. Erickson, J. Analytis, J.-H. Chu, D. J. Singh, Z. Hussain, T. H. Geballe, I. R. Fisher, and Z.-X. Shen, Nature (London) **455**, 81 (2008).

[5] C. Liu, G. D. Samolyuk, Y. Lee, N. Ni, T. Kondo, A. F. Santander-Syro, S. L. Bud'ko, J. L. McChesney, E. Rotenberg, T. Valla, A. V. Fedorov, P. C. Canfield, B. N. Harmon, and A. Kaminski, Phys. Rev. Lett. **101**, 177005 (2008).

[6] H. Ding, P. Richard, K. Nakayama, K. Sugawara, T. Arakane, Y. Sekiba, A. Takayama, S. Souma, T. Sato, T. Takahashi, Z. Wang, X. Dai, Z. Fang, G. F. Chen, J. L. Luo, and N. L. Wang, Europhys. Lett. **83**, 47001 (2008).

[7] D. V. Evtushinsky, D. S. Inosov, V. B. Zabolotnyy, A. Koitzsch, M. Knupfer, B. Buchner, G. L. Sun, V. Hinkov, A. V. Boris, C. T. Lin, B. Keimer, A. Varykhalov, A. A. Kordyuk, and S. V. Borisenko, Phys. Rev. B **79**, 054517 (2009).

[8] M. C. Boyer, Kamalesh Chatterjee, W. D. Wise, G. F. Chen, J. L. Luo, N. L. Wang, and E. W. Hudson, arXiv:0806.4400 (unpublished).

[9] Yi Yin, M. Zech, T. L. Williams, X. F. Wang, G. Wu, X. H. Chen, and J. E. Hoffman, arXiv:0810.1048 (unpublished).

[10] D. Hsieh, Y. Xia, L. Wray, D. Qian, K. Gomes, A. Yazdani, G. F. Chen, J. L. Luo, N. L. Wang, and M. Z. Hasan, arXiv:0812.2289 (unpublished).

[11] A. Ohtomo and H. Y. Hwang, Nature (London) **427**, 423 (2004).

[12] H. Chen, Y. Ren, Y. Qiu, Wei Bao, R. H. Liu, G. Wu, T. Wu, Y. L. Xie, X. F. Wang, Q. Huang, and X. H. Chen, Europhys. Lett. **85**, 17006 (2009).

[13] Jiun-Haw Chu, James G. Analytis, Chris Kucharczyk, and Ian R. Fisher, Phys. Rev. B **79**, 014506 (2009).

[14] F. Massee, Y. Huang, R. Huisman, S. de Jong, M. S. Golden, and J. B. Goedkoop, arXiv:0812.4536, (unpublished).

[15] A. Fanelsa, R. Schellenberg, F. U. Hillebrecht, E. Kisker, J. G. Menchero, A. P. Kaduwela, C. S. Fadley, and M. A. Van Hove, Phys. Rev. B **54**, 17962 (1996).

[16] F. Schaefers, M. Mertin, and M. Gorgoi, Rev. Sci. Instrum. **78**, 123102 (2007).

[17] Due to the extreme grazing incidence geometry necessary to better match the inelastic mean-free path length of the photoelectrons and the penetration depth of the hard x rays, it is unavoidable to also pick up signals from the sample mounting.

[18] H. Ding, K. Nakayama, P. Richard, S. Souma, T. Sato, T. Takahashi, M. Neupane, Y.-M. Xu, Z.-H. Pan, A. V. Federov, Z. Wang, X. Dai, Z. Fang, G. F. Chen, J. L. Luo, and N. L. Wang, arXiv:0812.0534 (unpublished).

[19] Although the hard x-ray and VUV valence-band spectra in Fig. 2(a) are taken with different temperatures, it was checked and confirmed that data taken at room temperature with VUV radiation did not differ significantly from the low-temperature data.

[20] J. J. Yeh and I. Lindau, At. Data Nucl. Data Tables **32**, l (1985). These listed values, used throughout this document, are values for the *atomic* PIXs and are not necessarily directly applicable to more complicated compounds but can be well used as an estimate to the real values.

[21] The literature spectrum of Fe (111) shown in Fig. 1(c) has a small satellite around a binding energy of 712 eV, which is due to the fact that these data were taken with a Mg $k\alpha$ lab source. This feature is thus not a property of the Fe(111)Fe 2p core-level line shape.

[22] We note that, due to the small angular acceptance of the SES100 analyzer, the k-space integration of the $h\nu$=125 eV spectra is over only part of the 2D Brillouin zone. The depicted spectra are integrated over 40% of the Brillouin zone area around Γ. Using a polar rotation of the sample it was checked and confirmed that integration around different parts of the Brillouin zone, for instance, $(\pi, 0)$, yielded very similar spectra.

[23] J. Wu, Ph. Phillips, and A. H. Castro Neto, Phys. Rev. Lett. **101**, 126401 (2008).

[24] D. R. Garcia, C. Jozwiak, C. G. Hwang, A. Fedorov, S. M. Hanrahan, S. D. Wilson, C. R. Rotundu, B. K. Freelon, R. J. Birgeneau, E. Bourret-Courchesne, and A. Lanzara, Phys. Rev. B **78**, 245119 (2008).

[25] G. A. Sawatzky, I. S. Elfimov, J. van den Brink, and J. Zaanen, arXiv:0808.1390 (unpublished).

[26] W. Malaeb, T. Yoshida, T. Kataoka, A. Fujimori, M. Kubota, K.

Ono, H. Usui, K. Kuroki, R. Arita, H. Aoki, Y. Kamihara, M. Hirano, and H. Hosono, J. Phys. Soc. Jpn., **77**, 093714 (2008).

[27] A. Koitzsch, D. Inosov, J. Fink, M. Knupfer, H. Eschrig, S. V. Borisenko, G. Behr, A. Köhler, J. Werner, B. Büchner, R. Follath, and H. A. Dürr, Phys. Rev. B **78**, 180506(R) (2008).

[28] E. Z. Kurmaev, R. G. Wilks, A. Moewes, N. A. Skorikov, Yu. A. Izyumov, L. D. Finkelstein, R. H. Li, and X. H. Chen, Phys. Rev. B **78**, 220503(R) (2008).

[29] M. K. Bahl and R. L. Watson, Surf. Sci. **54**, 540 (1976).

[30] S. Hüfner, *Photoelectron Spectroscopy* (Springer-Verlag, Berlin, 1995).

[31] M. C. Schabel, C. H. Park, A. Matsuura, Z. X. Shen, D. A. Bonn, X. Liang, and W. N. Hardy, Phys. Rev. B **57**, 6090 (1998); V. B. Zabolotnyy, S. V. Borisenko, A. A. Kordyuk, J. Geck, D. S.

Inosov, A. Koitzsch, J. Fink, M. Knupfer, B. Buchner, S. L. Drechsler, H. Berger, A. Erb, M. Lambacher, L. Patthey, V. Hinkov, and B. Keimer, *ibid.* **76**, 064519 (2007); M. A. Hossain, J. D. F. Mottershead, D. Fournier, A. Botswick, J. L. McChesney, E. Rotenberg, R. Liang, W. N. Hardy, G. A. Sawatzky, I. S. Elfimov, D. A. Bonn, and A. Damascelli, Nat. Phys. **4**, 527 (2008).

[32] D. E. Eastman, T.-C. Chiang, P. Heimann, and F. J. Himpsel, Phys. Rev. Lett. **45**, 656 (1980).

[33] A. B. McLean, Surf. Sci. Lett. **220**, L671 (1989); J. W. Davenport, R. E. Watson, M. L. Perlman, and T. K. Sham, Solid State Commun. **40**, 999 (1981); W. Mönch, *ibid.* **58**, 215 (1986).

[34] P. E. Gregory and W. E. Spicer, Phys. Rev. B **13**, 725 (1976); D. J. Chadi, Phys. Rev. B **18**, 1800 (1978).